

Structure, linear and non-linear optical properties of thin $\text{As}_x\text{Se}_{1-x}$ films

K. PETKOV, R. TODOROV, J. TASSEVA, D. TSANKOV^a

Central Laboratory of Photoprocesses "Acad. J. Malinowski", Bulgarian Academy of Sciences, Acad. G. Bonchev Str., bl. 109, 1113 Sofia, Bulgaria

^a*Institute of Organic Chemistry with Centre of Phytochemistry, Bulgarian Academy of Sciences, Acad. G. Bonchev St., bl. 9, 1113 Sofia, Bulgaria*

Amorphous $\text{As}_x\text{Se}_{100-x}$ thin films with different compositions ($28 \leq x \leq 60$) were deposited onto Si wafers and optical glass substrates BK-7 by thermal evaporation. The changes in the optical properties and structure of thin films as a function of the composition, film thickness and conditions of thermal evaporation and exposure to light were studied. Optical constants (refractive index, n , and absorption coefficient, α) and thickness, d , as well as the optical band gap, E_g , were determined using a method similar to Swanepoel's envelope method and two triple - TR_iR_m and TR_bR_m methods (for very thin films). Applying the Wemple and Di Domenico model, the dispersion energy, E_d , single-oscillator energy, E_o , and effective coordination number per cation, N_c , for the studied films were estimated. It was shown that the calculated values of n , k and E_g do not depend on the evaporation rate (0.2–25 nm/s), film thickness (50-1000nm) and other conditions of evaporation. The maximum value of n was found to be in thin $\text{As}_{40}\text{Se}_{60}$ films. After exposure to light, an increase in n and decrease in thin film's thickness and optical band gap was observed. We have found that E_o and N_c increase with increasing the Se-content. Non-linear parameters obtained by different formulae for prediction of non-linear absorption and refractive index were compared. A correlation between the non-linear refractive index and linear optical properties of As-Se thin films was demonstrated. The results of photo-induced changes in the infrared spectra of thermally deposited As-Se were interpreted in terms of the changes in the film structure due to the photopolymerization of As_4Se_4 molecular units and selenium chains into an As_2Se_3 glassy network. The great changes in n after exposure to light of As-rich films suggest an opportunity for applying the films examined as inorganic photoresists, in multi-layered structures and for producing Bragg gratings.

(Received July 5, 2009; accepted November 12, 2009)

Keywords: Thin films, Chalcogenide glasses, Optical properties, Nonlinear refractive index, IR spectroscopy

1. Introduction

Chalcogenide bulk glasses and thin films from the systems As-S and As-Se have been intensively studied in the last three decades because of their high transparency in the IR spectral range, photoinduced changes of their properties, and capability to be doped [1-5]. These glasses are good candidates for thermal and medical imaging [6], optical memories [7], bio-sensing [8] or telecommunications [9]. It is well known that under exposure to band gap light, amorphous chalcogenide films undergo some changes in their structure and optical properties, including Raman bands intensities and position [3-5]. The ability of optical writing and thermal erasing of structures, combined with transparency in the infrared region and high nonlinearity [10] makes chalcogenide glasses suitable for thin film optical applications. From the differential absorption and reflectivity IR spectra measurements it was found that the intensities of several absorption bands, corresponding to As-As vibrations are changed due to illumination [11]. Amorphous As_2S_3 and As_2Se_3 thin films are applied for model investigations of photostructural transformations in amorphous chalcogenide glasses [12 -14].

Recently, the interest in nonlinear optical properties of glasses increased since materials with high nonlinear refractive index, n_2 , can reduce the switching power in all-

optical switching devices. There are some experimental indications that amorphous chalcogenides have rather high non-linear optical properties and, hence, these materials are promising candidates as non-linear optical elements [15 -17]. The measurements have been carried out using Z-scan, four-wave mixing or optical third-harmonic generation techniques [15, 18, 19], which are not common in most laboratories.

Regardless of existing numerous papers on the properties of chalcogenide thin As - Se films in our view no a complex investigation of the optical properties of $\text{As}_x\text{Se}_{100-x}$ films with different thickness deposited at comparable conditions.

In this paper we report a comparative study of the optical properties of thin films from the systems As - Se. Our aim is to determine the influence of the As- content on the linear and non-linear optical properties of thin chalcogenide films as well as the changes in their structure after illumination.

2. Experimental

Glassy As-Se samples were prepared from elements of purity 99,999% by the method of melt quenching. The compositions of the bulk glasses and of the thin films were determined by scanning electron microscopy with an X-

ray microanalyser (Jeol Superprobe 733, Japan). Thin $\text{As}_x\text{Se}_{100-x}$ films ($x = 28, 33, 40, 45, 50, 55$ and 60) with different thicknesses were deposited onto non-absorbing optical glass BK7, graphite and two-side polished Si wafers by thermal evaporation from a Mo crucible under vacuum of $6\text{-}8 \cdot 10^{-6}$ Torr. The deposition rate was controlled using a piezocrystal monitor and was varied between 0.2 and 25 nm/s [20]. The substrate temperature during evaporation was $25\text{-}30^\circ\text{C}$ and the films were not annealed after deposition. The thin films were deposited under the same conditions on substrates for different measurements. Optical transmission and reflection measurements in the spectral range $400 - 2000$ nm were carried out using an UV-VIS-NIR spectrophotometer (Cary 05E, USA). The films were exposed to light by a halogen lamp (20 mW/cm²). The exposure time to saturation (i.e. the time beyond which the absorption edge did not change) was experimentally established for each sample. The optical constants of films thicker than 200 nm (refractive index, n , and absorption coefficient, k) and the film thickness (d) were calculated using Swanepoel's method [21] and a computer program developed by Konstantinov [22]. It processes the data from just one spectrophotometric measurement – that of the film transmission.

As a result, the refractive indices, and the thicknesses of the films were determined with an accuracy of 1% .

In the case of the amorphous chalcogenide glasses, the optical absorption coefficient, α , changes rapidly for the photon energies comparable to that of the band gap, E_g , giving rise to an absorption edge. At the highest values of the absorption coefficient, α , when the condition $\alpha d > 1$ is realized, α , should be calculated from the equation [23]:

$$T = (1 - R)^2 e^{-\alpha d} \quad (1)$$

where T is the transmittance, R is the reflectance, α is the absorption coefficient and d is the film thickness. According to Tauc's dependence, the absorption coefficient is connected with the photon energy by the equation

$$\alpha h\nu = B (h\nu - E_g)^2, \quad (2)$$

where B is a substance parameter, h is Planck's constant and ν is the frequency, E_g is the optical band gap.

For calculation of optical constants of very thin films ($50\text{-}150$ nm) a different method (the triple method proposed by Panayotov and Konstantinov [24, 25]) was applied. The latter operates three spectrophotometric measurements – T, R_f, R_m or T, R_b, R_m , where T is the transmission, R_f, R_b and R_m – the reflections from the front, the back side of the BK7 substrate, and from the same film, deposited on a metal (Si wafer) substrate, respectively. The accuracy of the triple methods in determination of d is $1\text{-}2$ nm [26]. Further, for a more precise estimation of n and k , double methods developed by Abeles and Theye [27] were applied. Since the correlation (1) is a permissible approximation where $\alpha d \gg 10^4$, we had to use Eq. (3) for determination of the linear absorption coefficient, α :

$$\alpha = 4\pi k / \lambda \quad (3)$$

The refractive index dispersion was analyzed, using the single-oscillator model, proposed by and named after Wemple & Di Domenico [28] (WDDM). According to the authors, the refractive index dispersion is given by the relation:

$$n^2(h\omega) - 1 = \frac{E_d E_0}{E_0^2 - \hbar^2 \omega^2} \quad (4)$$

where E_d and E_0 are the dispersion and the single-oscillator energy, respectively, \hbar is Planck's constant divided by 2π , and $\hbar\omega$ is energy of light. Wemple and DiDomenico show that E_d obeys the relation

$$E_d = \beta N_c Z_a N_e \quad (5)$$

where N_c is the coordination number of the cation nearest neighbour to the anion, Z_a - the formal valency of anion, N_e is the total number of valence electrons per anion; for covalent materials, $\beta = 0.37$ eV. Thus, E_d values could be used for intermolecular interaction estimation.

3. Results and discussion

3.1 X-ray microanalysis

We have studied in detail the influence of the composition and conditions of film preparation and

Table 1. Data for the element content of the bulk and thin film chalcogenide samples

| Composition | Bulk samples | Thin films |
|--------------------------------|--------------------------------|--------------------------------|
| $\text{As}_{28}\text{Se}_{72}$ | $\text{As}_{27}\text{Se}_{73}$ | $\text{As}_{29}\text{Se}_{71}$ |
| $\text{As}_{33}\text{Se}_{67}$ | $\text{As}_{32}\text{Se}_{68}$ | $\text{As}_{34}\text{Se}_{66}$ |
| $\text{As}_{40}\text{Se}_{60}$ | $\text{As}_{41}\text{Se}_{59}$ | $\text{As}_{41}\text{Se}_{59}$ |
| $\text{As}_{45}\text{Se}_{55}$ | $\text{As}_{44}\text{Se}_{56}$ | $\text{As}_{46}\text{Se}_{54}$ |
| $\text{As}_{50}\text{Se}_{50}$ | $\text{As}_{51}\text{Se}_{49}$ | $\text{As}_{51}\text{Se}_{49}$ |
| $\text{As}_{55}\text{Se}_{45}$ | $\text{As}_{56}\text{Se}_{44}$ | $\text{As}_{54}\text{Se}_{46}$ |
| $\text{As}_{60}\text{Se}_{40}$ | $\text{As}_{60}\text{Se}_{40}$ | $\text{As}_{61}\text{Se}_{39}$ |

light exposure on the optical properties of thin As - Se films in a wide compositional interval. Thin films were deposited from by thermal evaporation of bulk samples from the system $\text{As}_x\text{Se}_{100-x}$ ($x = 28, 33, 40, 45, 50, 55$ and 60 at %) at temperature $250 - 350^\circ\text{C}$, depending on the composition. Using X-ray microanalysis, we have found that the element content of bulk glasses as well as of the thin films from the system $\text{As}_x\text{Se}_{100-x}$ ($28 \leq x \leq 60$), is very close (within ± 1 at.%) to the expected composition (Table 1).

3.2. Optical properties of As-Se thin films

The optical constants of thin As-Se films and their photoinduced changes depending on the film composition, conditions of deposition and exposure to light were calculated from transmission measurements of layers (~ 700 nm thick). In Fig. 1 the plots of the optical

transmission of thin As-Se films vs. wavelength, before and after exposure to white light are presented. It is seen that the absorption edge is shifted to the higher wavelengths after illumination and the effect of photodarkening increases with the increase of the As-content in the films (for As-rich films $\Delta\lambda > 40$ nm at $T = 20$ %).

The compositional dependence of the refractive index, n at $\lambda = 1,55$ μm is shown in Fig. 2a. It is seen that n increases from 2.64 for $\text{As}_{28}\text{Se}_{72}$, passes through a maximum for the composition $\text{As}_{40}\text{Se}_{60}$ ($n = 2.68$), and reaches its minimum value ($n = 2.54$) for $\text{As}_{60}\text{Se}_{40}$. The photoinduced changes in n after illumination with white light depend on the film composition too. Fig. 2 b shows that the relative

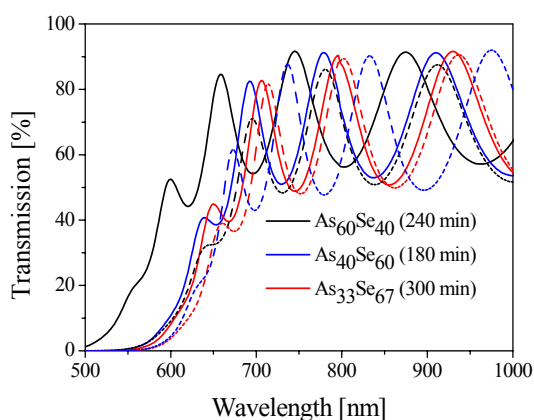


Fig. 1. Spectral dependence of the transmission of unexposed (—) and exposed (---) thin As-Se films. (In parentheses the exposure time to saturation is given).

deviation, $\Delta n/n$, of the refractive index at three fixed wavelength – 632.8, 1060 and 1550 nm increases with the increase of the As-content in the films—from 2 % for $\text{As}_{28}\text{Se}_{72}$ up to ~6 % for $\text{As}_{55}\text{Se}_{45}$ in the IR, and from 2.5 to 10 % in the range of strong absorption (at $\lambda = 632.8$ nm). The relative deviation of n is defined as:

$$\Delta n/n = (n_{\text{exp}} - n_{\text{unexp}})/n \quad (10)$$

where the subscripts „exp” and “unexp” mark the exposed and unexposed samples, respectively.

While the refractive index of thin As-Se films (Fig. 2a) has a maximum value for the composition $\text{As}_{40}\text{Se}_{60}$, the optical band-gap, E_g determined from the Eq. 2 shows a minimum value for the same composition (Fig. 3). A similar dependence of n and E_g is found for the $\text{As}_{40}\text{S}_{60}$ film from the system $\text{As}_x\text{S}_{100-x}$ [29]. The values of E_g and the slope of Tauc’s edge, B are presented in Table 2. It is seen that for unexposed layers, B decreases increasing the As-content which is connected with the disordering in the films. For exposed thin films B increases, which could mean that the width of the localized states decreases. As far as these states are due to the structural defects in the glassy matrix we could conclude the exposed films from

the system $\text{As}_x\text{Se}_{100-x}$ are structurally more ordered than as-deposited layers.

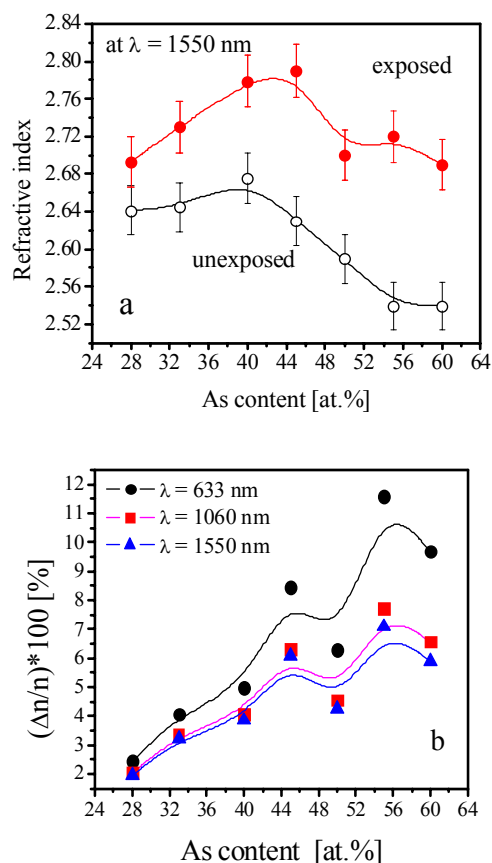


Fig. 2. Compositional dependence of the refractive index (a) and the relative deviation at $\lambda = 1.55$ μm (b) on the As-content of thin As-Se films. Lines are the guides to eye.

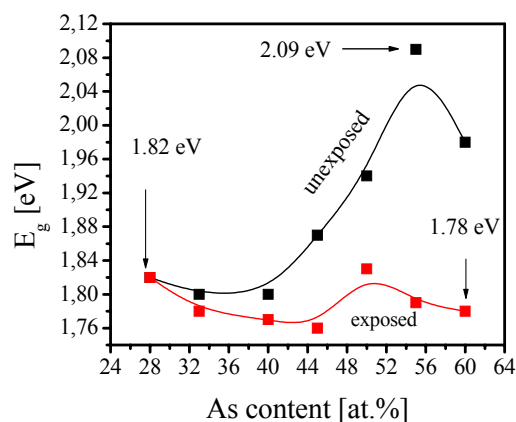


Fig. 3. Dependence of E_g of thin $\text{As}_x\text{Se}_{100-x}$ films on the As-content. Lines are the guides to eye.

Table 2. Data for the optical band-gap, E_g^{opt} and the slope of Tauc's edge, B for thin As_xSe_{100-x} films.

| Composition | E_0 [eV] | E_d [eV] | n_0 |
|------------------|---------------|---------------|-------|
| $As_{28}Se_{72}$ | 3.81 | 21.82 | 2.59 |
| $As_{33}Se_{67}$ | 3.86 | 21.78 | 2.59 |
| $As_{40}Se_{60}$ | 3.80 | 22.35 | 2.61 |
| $As_{45}Se_{55}$ | 3.88 | 21.90 | 2.58 |
| $As_{50}Se_{50}$ | 3.97 | 21.70 | 2.53 |
| $As_{55}Se_{45}$ | 4.27 | 22.65 | 2.50 |
| $As_{60}Se_{40}$ | 4.21 | 22.25 | 2.50 |

Using the Wemple–DiDomenico dispersion model [28] and Eq. (4), and plotting $(n^2 - 1)^{-1}$ against $(h\nu)^2$ we can determine the single-oscillator energy, E_0 and the dispersion energy, E_d by fitting a straight line to the experimental points, as shown in Fig. 4. It is seen that the experimental dispersion of the refractive index departs from the the Wemple–DiDomenico model [28] relates the dispersion energy, E_d , to other physical parameters of the material through the relationship given by Eq. (5). Therefore, according to this equation, any difference in E_d , as a consequence of the film composition, will be related to the differences in As effective coordination number, N_c .

The values of the dispersion parameters of As–Se thin films as well as the values of the static refractive index, $n(0)$, obtained by extrapolation of Eq. (4) towards $h\nu = 0$ are presented in Table 3. In Figs. 5 and 6 the compositional dependence of the cation coordination number, N_c and single-oscillator energy, E_0 are shown, respectively. As expected E_0 increases with the increase of As-content in the films and its maximum value was received to be for the composition $As_{55}Se_{45}$ (the same dependence was obtained for E_g) while N_c decreases increasing the As- content. This effect could be explained with the creation of As–As bonds in As-rich films.

Table 3. Data for the dispersion parameters of thin As–Se films.

| Composition | Unexposed | | Exposed | |
|------------------|------------------|----------------------------------|------------------|----------------------------------|
| | E_g^{opt} [eV] | B [$cm^{-1/2} eV^{-1/2}$] | E_g^{opt} [eV] | B [$cm^{-1/2} eV^{-1/2}$] |
| $As_{28}Se_{72}$ | 1.82 | 866 | 1.82 | 949 |
| $As_{33}Se_{67}$ | 1.80 | 795 | 1.78 | 833 |
| $As_{40}Se_{60}$ | 1.80 | 816 | 1.77 | 876 |
| $As_{45}Se_{55}$ | 1.87 | 785 | 1.76 | 828 |
| $As_{50}Se_{50}$ | 1.94 | 767 | 1.83 | 807 |
| $As_{55}Se_{45}$ | 2.09 | 770 | 1.79 | 772 |
| $As_{60}Se_{40}$ | 1.98 | 682 | 1.78 | 732 |

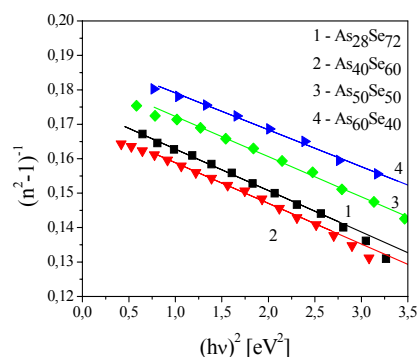


Fig. 4. Plot of the refractive-index factor $(n^2 - 1)^{-1}$ vs. $(h\nu)^2$ for unexposed amorphous As–Se films. Solid lines are the corresponding least-square linear fits.

The changes in the deposition conditions of thin films can lead to the formation of layers characterized by different structural states and physicochemical and optical properties. We investigated the influence of the deposition rate (evaporation temperature) and the film thickness on the optical properties of $As_{50}Se_{50}$ thin films. The results obtained are shown in Table 4 and Fig. 7.

It is evident that the refraction index, within the accuracy of the method applied, is independent of the evaporation rate. It might also be seen that the value of the optical band gap of unexposed thin $As_{50}Se_{50}$ film deposited with the highest rate (26.3 nm/s) considerably differs from the others ($E_g = 1.94$ eV, while for the layers deposited with lower deposition rate $E_g = 2.03$

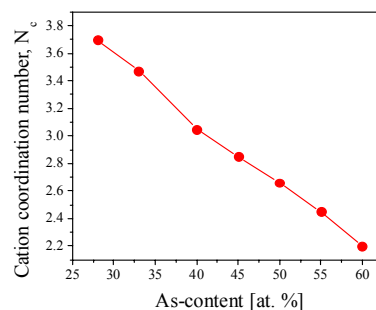


Fig. 5. Compositional dependence of the cation coordination number, N_c for As–Se thin films.

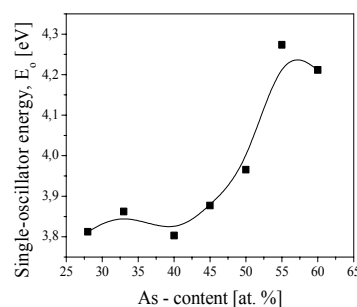


Fig. 6. Compositional dependence of the single-oscillator energy, E_0 for thin As_xSe_{100-x} films. The line is the guide to eye.

Table 4. Data for the optical parameters of thin $\text{As}_{50}\text{Se}_{50}$ films, depending on the deposition rate.

| Rate nm/s | Exposure | d [nm] | n (632.8 nm) | E_g [eV] |
|--------------|----------|-----------|-----------------|---------------|
| 0.19 | Unexp | 518 | 2.85 | 2.04 |
| | Exp | 514 | 3.14 | 1.78 |
| 0.52 | Unexp | 566 | 2.82 | 2.03 |
| | Exp | 551 | 3.08 | 1.81 |
| 0.73 | Unexp | 529 | 2.84 | 2.04 |
| | Exp | 526 | 3.08 | 1.80 |
| 26.3 | Unexp | 789 | 2.88 | 1.94 |
| | Exp | 787 | 3.04 | 1.81 |

eV). This effect could be associated with the process of film's growth. It seems that such films are more inhomogeneous and defect states are formed in the band-gap. After exposure to light no difference in the values of the optical band-gap – all layers are more ordered. For the needs of our research, where deposition rate has been confined to low values, the assertion of independence is acceptable.

The photo-induced increase in n between 6 and 10 % gives a possibility for grating production.

3.3. Optical properties of very thin films

The multi-layer structures are of great interest for optoelectronics. This stimulates us to examine to what extent the thickness affects the properties of the films. Optical constants of very thin films (50-100 nm thick) were calculated from the optical transmission and reflection from the front, the back side of the BK7 substrate, and from the same film, deposited on a Si wafer substrate [26]. We have found that for the composition $\text{As}_{28}\text{Se}_{72}$, the absorption edge shift and the changes in the refractive index after exposure to light are negligible (< 5 nm and < 0.02 , respectively) [30]. That is why we have not performed experiments on this composition. Comparing the shift of the absorption edge in films with composition $\text{As}_{40}\text{Se}_{60}$ and $\text{As}_{50}\text{Se}_{50}$, we could conclude that $\text{As}_{50}\text{Se}_{50}$ films ($\Delta\lambda = 50-60$ nm) are more sensitive to light illumination than those of the $\text{As}_{40}\text{Se}_{60}$ ones ($\Delta\lambda = 25-35$ nm) [20].

The dispersion of the refractive index at different wavelengths for thin $\text{As}_{40}\text{Se}_{60}$ and $\text{As}_{50}\text{Se}_{50}$ films (about 80 nm thick) is shown in Fig. 8. The values of n for unexposed $\text{As}_{40}\text{Se}_{60}$ films are higher than those for $\text{As}_{50}\text{Se}_{50}$ layers and the photoinduced increase in n at 1500 nm is $\Delta n = 0.2$ for the first composition. Fig. 9 illustrates the influence of the thickness of the above thin films on the dispersion of n . We have compared three layers of different thickness (32, 88, 117 nm). At $\lambda > 700$ nm, the refractive index of the film, 88 nm thick, perfectly matches the one of 117 nm. The average increase of n at $\lambda = 632.8$ nm is 10 % for the three values of d . That is an evidence about sensitivity independence on films' thickness.

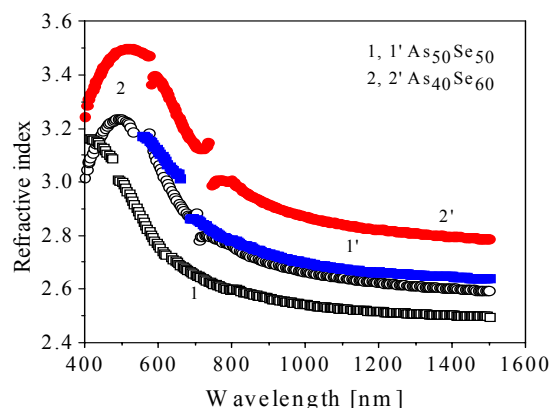


Fig. 8. Dispersion of the refractive index of unexposed (1,2) and exposed (1', 2') thin $\text{As}_{50}\text{Se}_{50}$ (1, 1') and $\text{As}_{40}\text{Se}_{60}$ (2, 2') films (about 80 nm thick).

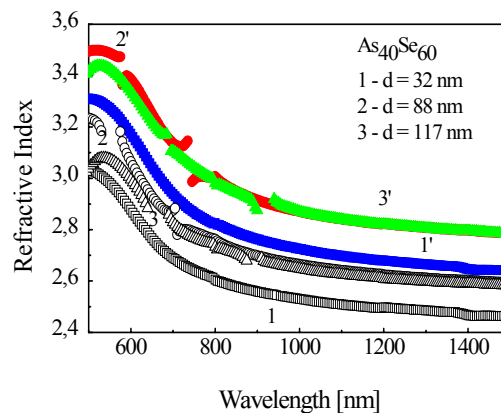


Fig. 9. Dispersion of the refractive index of unexposed (1-3) and exposed (1'-3') thin $\text{As}_{40}\text{Se}_{60}$ films with different thickness.

The refractive index of the film, 32 nm thick, considerably differs from the index dispersions of the thicker layers. The above results are in agreement with previous reports, which claim the existence of a critical value for d , above which optical constants are thickness independent [31].

Fig. 10 shows the variations in the refractive index of thin $\text{As}_{50}\text{Se}_{50}$ depending on the film thickness. We have shown here only data for unexposed and exposed $\text{As}_{50}\text{Se}_{50}$ films but we have observed the same effect on thin films with other compositions. The average values of n after illumination by light increase by 8 %. It is seen that in the limits of precision of the refractive index determination, n of thin $\text{As}_{50}\text{Se}_{50}$ films does not depend on the film thickness (for layers thicker than 80 nm). It is evident that a critical film thickness exists and for thinner films because of the island inhomogeneous structure of coatings some errors in calculation of the optical constants arise.

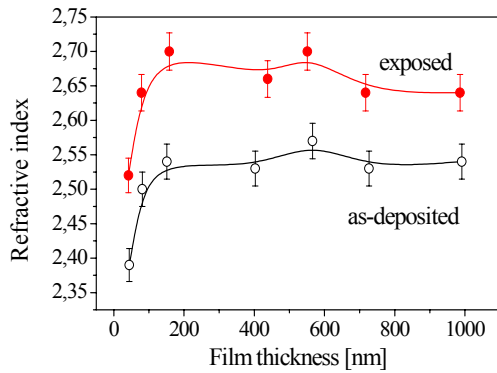


Fig. 7. Variation in the refractive index of thin $As_{50}Se_{50}$ films at $\lambda = 1550$ nm from the film thickness. Lines are the guides to eye.

On Fig. 11, we have compared the shift of the absorption edge for three layers of thin $As_{50}Se_{50}$ films with various thickness – 44, 81, 151 nm. It is shown that the values for the optical band gap differ insignificantly from one another.

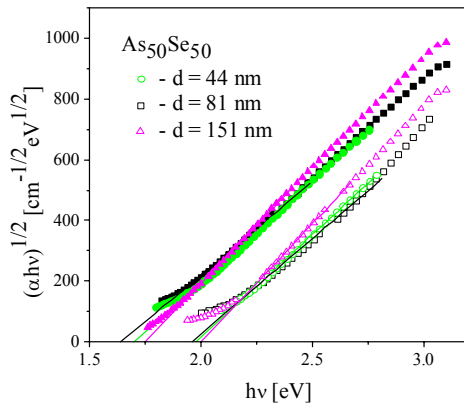


Fig. 11. Absorption edge shift of unexposed (open symbols) and exposed (full symbols) thin $As_{50}Se_{50}$ films with different thickness.

3.4 Non-linear optical properties of thin As -Se films

For prediction of the non-linear refractive index, we have applied a formula developed by Sheik-Bahae et al. [32]. In the simple model, γ can be expressed as:

$$\gamma = K \frac{\hbar c \sqrt{E_p}}{2n^2 E_g^{opt4}} G_2(\hbar\omega / E_g^{opt}) \quad (6),$$

where $E_p = 21$ eV, K is found to be 3.1×10^{-8} in units such that E_p and E_g^{opt} are measured in eV, and γ is measured in

m^2/W , \hbar – Planck's constant divided by 2π , c the speed of light in a vacuum and G_2 - a universal function:

$$G_2(x) = \frac{-2 + 6x - 3x^2 - x^3 - \frac{3}{4}x^4 - \frac{3}{4}x^5 + 2(1-2x)^{3/2}\Theta(1-2x)}{64x^6} \quad (7)$$

where Θ is the Heaviside step function. n_2 and γ are related by:

$$n_2 [esu] = \frac{cn}{40\pi} \gamma [SI] \quad (8)$$

The second formula for predicting the non-linear refractive index, n_2 , from linear refractive index at long wavelengths, n , which expresses n_2 in terms of the single oscillator energy, E_0 , and the dispersion energy, E_d , of the Wemple-DiDomenico model used by us is developed by Petkov and Ewen [33]:

$$n_2 = \frac{\sqrt{3gS(n^2+2)^{1.5} (n^2-1)^2 \hbar^2 e^2}}{12nmE_d E_0^2} \quad (9)$$

where g is the inharmonicity parameter, S - the oscillator strength, \hbar – Planck's constant divided by 2π , e and m being the electron charge and mass respectively. The results are presented in Table 5.

Table 5. Non-linear optical properties of as-deposited As-Se thin films.

| Composition | $\lambda=1550$ nm | | n_2 [esu] $\times 10^{-11}$ Petkov-Ewen [33] | γ_2/γ_2 SiO ₂ |
|------------------|---|------------------------------------|--|--------------------------------------|
| | γ [m^2/W] $\times 10^{-18}$ [32] | n_2 [esu] $\times 10^{-11}$ [32] | | |
| $As_{28}Se_{72}$ | 6.56 | 4.14 | 3.04 | 239 |
| $As_{33}Se_{67}$ | 7.00 | 4.42 | 2.94 | 255 |
| $As_{40}Se_{60}$ | 6.61 | 4.22 | 3.18 | 241 |
| $As_{45}Se_{55}$ | 5.64 | 3.54 | 2.84 | 206 |
| $As_{50}Se_{50}$ | 4.72 | 2.92 | 2.49 | 172 |
| $As_{55}Se_{45}$ | 3.28 | 1.99 | 1.89 | 120 |
| $As_{60}Se_{40}$ | 4.38 | 2.66 | 1.98 | 160 |

From Table 5 we can conclude that the non-linear refractive index, n_2 , increases with the increase of Se-content in the films passing through a maximum for films with composition $As_{33}Se_{67}$ according to Eq. (8) or $As_{40}Se_{60}$, according to Eq. (9). These data are comparable with the values presented in [34]. It is also seen that n_2 of As-Se thin films is more than 120-250 times higher than that of fused silica. The value of non-linear refractive index of thin $As_{40}Se_{60}$ film found by Hajto et al [35] is 2.35×10^{-11} esu which is close to that obtained by us using

Eq. (9). In [16] the result from measurements of γ at $\lambda = 1550$ nm for As_2Se_3 showed that n_2 was calculated to be 295 times higher than that of silica. According to Eq. (6) the non-linear refractive index is strongly dependent on the optical band gap, and since enriching the film composition with Se narrows the band gap (Table 2), the observance above is absolutely expected.

We have found a certain agreement between the values of n_2 , calculated according to the formulae of Sheik-Bahae [32] and the one developed by Petkov and Ewen [33].

In [36] the non-linear refractive index, n_2 , of new germanium-based sulfo-selenide glasses has been measured at $\lambda = 1064$ nm using Z-scan technique and has been shown that the value of n_2 strongly increases with the substitution of S by Se, up to 350 times the n_2 for fused silica. n_2 was found to be 5 times higher for 70 at. % Se compared with that for 70 at. % s in the glasses.

As a tendency our results on thin films are in agreement with other results published until now for bulk chalcogenide glasses for which the ratio between the values of n_2 of chalcogenides and that for fused silica is higher. [37].

The obtained increase of the non-linear refractive index with exposure to light is apparently related to photoinduced irreversible changes of film structure.

3.5 IR spectra of thin $\text{As}_x\text{Se}_{100-x}$ films

The method of FTIR spectroscopy was applied for studying photoinduced changes in the structure of thin chalcogenide films depending on film composition. The IR spectra of thin $\text{As}_x\text{Se}_{100-x}$ films ($0 \leq x \leq 60$) (about 1 μm thick), deposited on double polished Si wafers have been measured before and after exposure to light for the same time as the film on the BK-7 substrates. The IR spectra are shown in Figs.12 and 13. It is shown that the main vibrational bands of the films from the studied system are grouped in a narrow spectral region of 200 – 270 cm^{-1} . Strong absorption peaks at 222, 226, 234 and 245 cm^{-1} , together with some lower-intensity peaks at 148, 156, 168, 172, 203, 260, 276, 289 and 304 cm^{-1} were observed in the as-deposited layers.

In Fig. 12a it is seen that for unexposed $\text{As}_{28}\text{Se}_{72}$ film three strong peaks exist: at 224 cm^{-1} (due to AsSe_3 vibrations) and at 240 and 276 cm^{-1} (assigned to Se-Se bridges between AsSe_3 pyramidal units and As_4Se_4 or As_4Se_3 cages). Due to Se, the fundamental vibrations at 245 cm^{-1} of AsSe_3 pyramids are shifted towards lower frequencies (223 and 234 cm^{-1}).

When the concentration of As increases, there is a shift of the band at 224 cm^{-1} to higher wavenumbers (234 and 245 cm^{-1}) showing a larger number of As-Se and As-As bonds (connected with the crystal As_4Se_4) the glassy network compared to that of $\text{As}_{28}\text{Se}_{72}$ which is expected to have a larger number of Se-Se bonds (Figs. 12b, c and 13). For thin $\text{As}_{60}\text{Se}_{40}$ film it is seen that the band at 245 cm^{-1} becomes very sharp and many small peaks appear (197,

218 224 cm^{-1}). That means some crystallization exists in the $\text{As}_{60}\text{Se}_{40}$ thin films.

In the As-Se films, the effect of light irradiation the change of the absorption spectra is small for thin films with compositions $\text{As}_{60}\text{Se}_{40}$ and $\text{As}_{28}\text{Se}_{72}$. Only a shift to the smaller wavenumbers was registered. For thin $\text{As}_{40}\text{Se}_{60}$ and $\text{As}_{50}\text{Se}_{50}$ films we have observed an increase in vibrational band intensity for As-Se bonds (222 cm^{-1}) proper to symmetric valence As-Se vibrations in pyramidal AsSe_3 units [38-40], as well as a decrease of homopolar bonds vibrations at 234 cm^{-1} (As-As bonds). Our results are similar with those received IR Fourier Spectroscopy and published in [38-40].

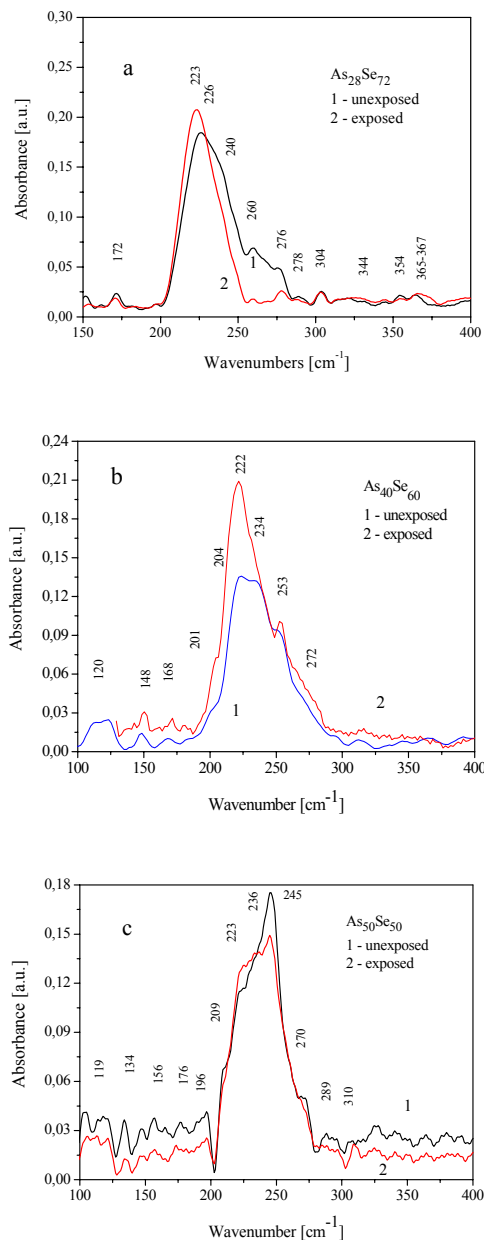


Fig. 12. IR spectra of unexposed and exposed thin $\text{As}_{28}\text{Se}_{72}$ (a), $\text{As}_{40}\text{Se}_{60}$ (b) and $\text{As}_{50}\text{Se}_{50}$ (c) films.

Irreversible photo-induced changes in the structure of As-Se thin films correspond to homopolar As-As and Se-Se bonds switching into heteropolar As-Se ones.

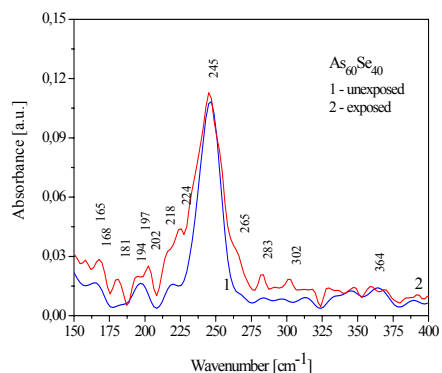


Fig. 13. IR spectra of unexposed and exposed thin $As_{60}Se_{40}$ films.

4. Discussion

Thin films of chalcogenide glasses represent inorganic polymers with a specific branched polymer structure. According to some authors, the vapor phase during the process of evaporation of As-Se glasses is a heterogeneous mixture of structural units of type As_2Se_3 , As_4Se_4 , As_4 and Se_8 . On the glass substrates some of them recombine but it is very likely that some units could be found in the deposited thin films forming some homopolar bonds (As-As, Se-Se). On illumination, polymer destructive changes occur leading to weakening of some bonds and to strengthening of others. The existence of photoinduced structural changes in these films is supported by changes in the physico-chemical properties (microhardness and T_g) as well as their optical properties.

Our experiments showed that the values of the absorption edge shift ($\Delta\lambda$), Δn and ΔE_g are like those published in the literature until now and in some cases are higher.

It is well known [41,42] that the structure of the As-containing binary amorphous chalcogenides consists of locally two-dimensional structural layers, formed by $AsS(Se)_3$ pyramidal units linked through common two-fold coordinated chalcogen atoms, and interacting with each other by weak intermolecular bonds. According to Wemple, interactions between structural layers through As atoms acting as bonding points, forming $As \dots S(Se)$ intermolecular bonds, would contribute to increase the As effective coordination number, and thus $N_c > 3$ is expected.

Using spectrophotometric measurements we have calculated the refractive index, n and thickness, d of thin chalcogenide films from the system As-Se. Applying single, double and triple methods established in the Laboratory optical properties of thin films with different thickness were determined and it was found that the optical constants do not depend on film thickness in the range of 50-100 nm and the rate of film deposition (0.19-25 nm/s). According to [44] vapour of As_2S_3 consist of different sulfur or arsenic rich fractions of the type As_2S_3 ,

As_4S_3 , As_4S_4 , As_4S_8 , S_8 during thermal evaporation. It could be supposed that in the case of evaporation of glasses from this system similar clusters with selenium are produced.

The structural investigations of as-deposited As-Se thin films suggest that the film consists of As_4Se_6 molecular units, molecular As_4Se_4 units or combination of As_2Se_3 , As_4Se_3 , As_4Se_4 , As_4 and chains or rings Sm ($m = 1-8$). Therefore, as-deposited thin films consist of clusters with heteropolar As-Se and homopolar As-As and Se-Se bonds. On illumination, changes in the polymer network lead to weakening of some bonds and to strengthening of others.

The presence of As_4Se_4 units is responsible for the appearance of peaks at and in the IR spectra, and the $AsSe_3$ pyramids for the peak at 222 cm^{-1} . On illumination some changes in the intensity of peaks at 222, 234 and 245 cm^{-1} occur. The irreversible changes occurring after exposure of as-deposited films are accompanied by a density increase of the As-Se bonds, i.e. a photopolymerization process of As_4Se_6 molecules. This leads to an increase in refractive index, decrease in the optical band-gap and changes in the absorption peaks at obtained by infrared spectroscopy [38].

The illumination of the films leads to stabilization of the local structure through redistribution of chemical bonds of the nearest environment. The interaction between As and Se rich molecular fragments takes place with the increase in the number of $AsSe_{3/2}$ structural units.

The results for the thickness changes in thin As-Se films demonstrated a decrease of the effect of exposure to light increasing the Se-content in the films. The relative changes in the thickness $\Delta d/d$ is -4% for $As_{40}Se_{60}$ thin films, i.e. an effect of photocontraction was observed.

5. Conclusions

Thin homogeneous chalcogenide As-Se films with compositions close to those of the synthesized bulk glasses were deposited by thermal evaporation. The optical characterization of the thin films was carried out by using single, double and triple methods established in the Laboratory. It was found that the optical constants do not depend on film thickness in the range of 50-100 nm and the rate of film deposition (0.19 – 25 nm/s). From spectrophotometric measurements, the optical constants and thicknesses of the layers were determined. It was found that the linear refractive index, n increases from 2.64 for $As_{28}Se_{72}$, passes through a maximum for the composition $As_{40}Se_{60}$ ($n = 2.68$), and reaches its minimum value ($n = 2.54$) for $As_{60}Se_{40}$. The relative deviation, $\Delta n/n$, increases with the increase of As-content in the films. While the refractive index of thin As-Se films has a maximum value for the composition $As_{40}Se_{60}$, the optical band-gap, E_g , shows a minimum value for the same composition.

The transmittance measurements of the chalcogenide As-Se films showed that after exposure to light the absorption edge was shifted to the longer wavelengths (an effect of photo-darkening). The highest value of the shift was $\Delta\lambda = 60 \text{ nm}$ (at $T = 20 \%$) for the composition $As_{50}Se_{50}$. After exposure to light to saturation degree, we observed a significant increase of the refractive index at λ

= 1550 nm (by 0.18, or 8 % for $\text{As}_{55}\text{Se}_{45}$) and a decrease in the band gap with 0.3 eV.

The non-linear refractive index, n_2 , increases with the increase of Se-content in the films passing through a maximum for films with composition $\text{As}_{33}\text{Se}_{67}$ according to Eq. (8) or $\text{As}_{40}\text{Se}_{60}$, according to Eq. (9). We have also found a certain agreement between the values of n_2 , calculated according to the formulae of Sheik-Bahae and the one developed by Petkov and Ewen.

The photo-induced change in the optical properties of chalcogenide thin films depending on the film composition and exposure to light is accompanied by changes in their structure.

Acknowledgement

The authors would like to acknowledge the financial support of the national Scientific Found (Contract 1314/2004 and Contract D002-123/2008) and J. Pirov for the X-ray microanalysis of bulk samples and thin films.

References

- [1] S. R. Elliott, *Physics of Amorphous Materials*, 2nd Edition, Longman, Essex, 1990.
- [2] Ke. Tanaka, *Rev. Solid State Sci.* **4**, 641 (1990).
- [3] P. J. S. Ewen, A. E. Owen, in *Hig- Performance Glasses*, (Cable M. and J.M. Parker, Editors), Blsckie, London, pp. 287-308 (1992).
- [4] M. Frumar, M. Vlcek, Z. Cernosek, Z. Polak, B. Frumarova, in *Physics and Application of Non-Crystalline Semiconductors in Optoelectronics*, Proc. NATO Workshop, Kishinev, Kluwer Acad. Publ., (Andries A. and M. Bertolotti, Editors), London, 1997, pp. 123-139.
- [5] A.V. Kolobov, Ed., *Photo-induced Metastability in Amorphous Semiconductors*, Wiley-CH, Weinheim, 2003.
- [6] B. Bureau, X.H. Zhang, F. Smectala, J.L. Adam, J. Troles, C. Boussard-Pledel, J. Lucas, P. Lucas, D. Le Coq, M.R. Riley and J.H. Simmons, *J. Non-Cryst. Solids* **345**, 276 (2004).
- [7] A.V. Kolobov, J. Tominaga, *J. mater. Sci. Mater. Electron.* **14**, 677 (2003).
- [8] P. Lucas, D. le Coq, C. Juncker, J. Collier, D. E. Boesewetter, C. Boussard-Pledel, B. Bureau, M.R. Riley, *Appl. Spectrosc.* **59**, 1 (2005).
- [9] M. Assobe, T. Kanamori and K. Kubodera, *IEEE J. Quantum Electron.* **29**, 2325 (1993).
- [10] G. Lenz, J. Zimmermann, T. Katsufuji, M. E. Lines, H. Y. Hwang, S. Spalter, R. E. Slusher, S.-W. Cheong, *Opt. Lett.* **25**, 254 (2000).
- [11] O.I. Shpotyuk., *Phys. Status Solidi B* **183**, 365 (1994).
- [12] S. A. Solin, G. N. Papatheodorou, *Phys. Rev.* **B15**, 2084 (1977).
- [13] U. Strom, T. P. Martin, *Solid State Commun.* **29**, 527 (1979).
- [14] E. V. Shkolnikov, V. S. Gerasimenko, Z.U. Borisova, *Fiz. Khim. Stekla* **3**, 338 (1977).
- [15] H. Nasu, Y. Ibara, K. Kubodera, *J. Non-Cryst. Solids* **110**, 353 (1989).
- [16] T. Cardinal, K.A. Richardson, H. Shin, A. Schutte, R. Beatty, K.I. Foulgoe, C. Meneghini, J.F. Viens, A. Villeneuve, *J. Non-Cryst. Solids* **256/257**, 353 (1999).
- [17] F. Smectala, C. Quemard, V. Couderac, A. Barthelemy, J. Lucas, *J. Phys. Chem.. Solids* **62**, 1435 (2001).
- [18] M. Sheik-Bahae, A. A. Said, Tai-Huei Wei, D. J. Hagan, E. W. Van Stryland, *IEEE J. Quantum Electron.* **26** (4), 760 (1990).
- [19] D. W. Hall, N. F. Borrelli, W. H. Dumbaugh, M. A. Newhouse and D.L. Weldmann, *Proc. Symp. Nonlin. Opt. Mat. Troy* (1988) 293.
- [20] J. Tasseva, R. Todorov, K. Petkov, *Nanoscience & Nanotechnology*, **5**, 1 (2005), Eds. E. Balabanova, I. Dragieva, Heron Press, Sofia.
- [21] R.J. Swanepoel, *Phys. E* **16**, 1214 (1983).
- [22] I. Konstantinov, private communication.
- [23] Tauc, *Amorphous and Liquid Semiconductors*, Chapter 4, New York, Plenum (1974).
- [24] V. Panayotov, I. Konstantinov, *Proc.SPIE* **2253**, 1070 (1994).
- [25] V. Panayotov, I. Konstantinov, *Bulg. Chem. Commun.* **26**, 612 (1993).
- [26] R. Todorov, K. Petkov, *J. Optoelectron. Adv. Mater.* **3**, 311 (2001).
- [27] F. Abeles, M. Theye, *Surf. Sci.* **5**, 325 (1966).
- [28] S.H. Wemple, M. DiDomenico, Jr., *Phys. Rev.* **B 3** (4), 1338 (1971).
- [29] K. Tanaka, *Thin Solid Films* **66** 271 (1980).
- [30] S. B. Gurevich, N. N. Ilyashenko, B. T. Kolomietz, V. M. Lyubin, V. P. Shilo, K. Hauashi, N. Mitsuishi, *J. Non-Cryst. Solids* **326 & 327**, 263 (2003).
- [31] K. Shimakawa, A. Ganjoo, *J. Optoelectron. Adv. Mater.* **3**, 167 (2001).
- [32] M. Sheik-Bahae, D. J. Hagan, E. W. Van Stryland, *Phys. Rev. Lett.* **65**, 96 (1990).
- [33] K. Petkov, P. J. S Ewen, *J. Non-Cryst. Solids* **249** 150 (1999).
- [34] J. Tasseva, R. Todorov, K. Petkov, *J. Optoelectron. Adv. Mater.* **11** (9), 1257 (2009).
- [35] E. Hajto, P.J.S. Ewen and A.E. Owen, *J. Non-Cryst. Solids* **164-166**, 901 (1993).
- [36] L. Petit, N. Carble, A. Humeau, G. Boudebs, H. Jain, A. C. Miller, K. Richardson, *Mater. Res. Bull.* **42** 2107 (2007).
- [37] J. S. Sanghera, C. M. Florea, L. B. Shaw, P. Pureza, V. Q. Nguyen, M. Bashkansky, Z. Dutton, I. D. Aggarwal, *J. Non-Cryst. Solids* **354**, 462 (2008).
- [38] O. I. Shpotyuk, *Opto-electronics Review* **11**(1), 19 (2003).
- [39] A. M. Shkolnikova, V. S. Gerasimenko, E.V. Shkolnikov, *Fiz. Khim. Stekla* **8**, 497 (1982) (in Russian).
- [40] E. V. Shkolnikov, V. S. Gerasimenko, Z. U. Borisova, *Fiz. Khim. Stekla* **3**, 338 (1977).
- [41] S. R. Elliott, *Physics of Amorphous Materials*, second ed., Longman, Lomdon, 1990.
- [42] Ke. Tanaka, *J. Phys. Chem. Solids* **68**, 896 (2007).
- [43] S. H. Wemple, *Phys. Rev.* **B7**, 3767 (1973).
- [44] T. P. Martin, *J. Phys. Chem.* **80** 170 (1984).